Catalysis of Hydrolysis and Transesterification Reactions of *p*-Nitrophenyl Esters by a Designed Helix−Loop−Helix Dimer

Kerstin S. Broo, Lars Brive, Per Ahlberg, and Lars Baltzer*

Contribution from the Department of Organic Chemistry, Göteborg University, 412 96 Göteborg, Sweden

Received March 17, 1997[⊗]

Abstract: KO-42, a polypeptide with 42 amino acid residues has been designed to fold into a hairpin helix−loop−helix motif that dimerizes and forms a four-helix bundle. The solution structure of the folded KO-42 dimer has been determined by NMR and CD spectroscopy and ultracentrifugation. On the surface of the folded polypeptide a reactive site has been engineered that is capable of catalyzing acyl-transfer reactions of reactive esters. The reactive site of KO-42 contains six histidine residues with perturbed pK_a values. The pK_as of His-15, His-30, and His-34 are close to 5, whereas those of His-11, His-19, and His-26 are close to 7, with nonideal titration curves. The second-order rate constant for the KO-42 catalyzed hydrolysis of mono-*p*-nitrophenyl fumarate at pH 4.1 and 290 K is 0.1 M^{-1} s^{-1}, which is 1140 times larger than that of the 4-methylimidazole (4-MeIm) catalyzed reaction, 8.8×10^{-5} M^{-1} s^{-1}. The second-order rate constant for the KO-42 catalyzed transesterification of mono-*p*-nitrophenyl fumarate to form the corresponding trifluoroethyl ester in 10 vol % trifluoroethanol at pH 4.1 and 290 K is 0.052 M^{-1} s^{-1} which is 620 times larger than that of the 4-MeIm catalyzed reaction, 8.4×10^{-5} M^{-1} s^{-1}. KO-42 catalyzes the corresponding reactions of other *p*-nitrophenyl esters with similar rate enhancements. At pH 4.1 in aqueous solution where the rate constant ratio k_2(KO-42)/k_2(4-MeIm) is larger than 10^3 the predominant reactive species of KO-42 have unprotonated histidines flanked by protonated histidines. The kinetic solvent isotope effect at pH 4.7 is 2.0 which shows that isotopic fractionation occurs in the transition state. The kinetic solvent isotope effect at pH 6.1 is 1.1 which shows that there is neither general acid−general base catalysis nor strong hydrogen bonding in the transition state of the rate-limiting reaction step at that pH. The results suggest that at low pH the dominant catalytic species functions through a mechanism where unprotonated nucleophilic histidines are flanked by protonated histidines that bind to one or both of the ester oxygens in the transition state.

Introduction

De novo designed proteins[1,2] have great potential in the engineering of novel catalysts because natural as well as non-natural amino acids can be organized in three-dimensional space to form complex reactive sites if the structure of the folded peptide can be predicted. Designed four-helix bundles,[1,3−6] β-sandwich proteins,[7] and a $\beta\beta\alpha$ motif[8] have been reported to fold in solution, and the formation of well-defined tertiary structures has recently been demonstrated by NMR and CD spectroscopy.[3,5,8] The introduction of reactive sites on the surface of folded polypeptides is therefore timely, and the engineering of hydrophobic cavities can now be envisioned using, e.g., novel reactions for the posttranslational modification of proteins.[9]

Designed polypeptide catalysts have been reported previously,[10−12] but it is only in a few cases where the relationship between structure and reactivity is at least partly understood. Oxaldie,[11] a peptide with 14 amino acid residues that aggregates and forms amphiphilic helices, was reported to catalyze the decarboxylation of oxaloacetate with a second-order rate constant that was almost three orders of magnitude larger than that of the ethyl amine catalyzed reaction. The secondary structure was identified by NMR and CD spectroscopy, but the tertiary structure could not be determined due to the dynamic nature of the helical aggregate. A designed four-helix bundle with a chymotrypsin-like active site was reported[12] to catalyze the hydrolysis of *p*-nitrophenyl acetate with a substantial rate enhancement, but the active site was later found not to function as intended.[13]

We recently reported on the reactivity of functionalized helix−loop−helix dimers[9,14,15] where the reactive sites were based on histidines flanked by residues capable of transition state binding. The reactive polypeptides were developed from SA-42, a designed polypeptide that folded into a hairpin helix−loop−helix motif and dimerized to form a four-helix bundle.[4] The solution structure was determined by NMR and CD spectroscopy and ultracentrifugation, and SA-42 was found to form the designed motif.[4,16] The solution structures of the

[⊗] Abstract published in *Advance ACS Abstracts,* November 1, 1997.

(1) Bryson, J. W.; Betz, S. F.; Lu, H. S.; Suich, D. J.; Zhou, H. X.; O'Neill, K. T.; DeGrado, W. F. *Science* **1995**, *270*, 935.
(2) Mutter, M.; Vuilleumier, S. *Angew. Chem., Int. Ed. Engl.* **1989**, *28*, 535.
(3) Raleigh, D. P.; Betz, S. F.; DeGrado, W. F. *J. Am. Chem. Soc.* **1995**, *117*, 7558.
(4) Olofsson, S.; Johansson, G.; Baltzer, L. *J. Chem. Soc., Perkin Trans. 2* **1995**, 2047.
(5) Dolphin, G. T.; Brive, L.; Baltzer, L. *J. Am. Chem. Soc.* **1996**. *118*, 11247.
(6) Fezoui, Y.; Weaver, D. L.; Osterhout, J. J. *Proc. Natl. Acad. Sci. U.S.A.* **1994**, *91*, 3675.
(7) Quinn, T. P.; Tweedy, N. B.; Williams, R. W.; Richardson, J. S.; Richardson, D. C. *Proc. Natl. Acad. Sci. U.S.A.* **1994**, *91*, 8747.
(8) Struthers, M. D.; Cheng, R. P.; Imperiali, B. *Science* **1996**,*271*, 342.
(9) Broo, K.; Brive, L.; Lundh, A.-C.; Ahlberg, P.; Baltzer, L. *J. Am. Chem. Soc.* **1996**, *118*, 8172.
(10) Gutte, B.; Daeumigen, M.; Wittschieber, E. *Nature* **1979**, *281*, 650.
(11) Johnsson, K.; Allemann, R. K.; Widmer, H.; Benner, S. A. *Nature* **1993**, *365*, 530.
(12) Hahn, K. W.; Klis, W. A.; Stewart, J. M. *Science* **1990**, *248*, 1544.
(13) Corey, M. J.; Hallakova, E.; Pugh, K.; Stewart, J. M. *Appl. Biochem. Biotechnol.*, **1994**, *47*, 199.
(14) Baltzer, L.; Lundh, A.-C.; Broo, K.; Olofsson, S.; Ahlberg, P. *J. Chem. Soc., Perkin Trans. 2* **1996**, 1671.
(15) Broo, K.; Allert, M.; Andersson, L.; Erlandsson, P.; Stenhagen, G.; Wigström, J.; Ahlberg, P.; Baltzer, L. *J. Chem. Soc., Perkin Trans. 2* **1997**, 397.
(16) Olofsson, S.; Baltzer, L. *Folding Design* **1996**. *1*, 347.

S0002-7863(97)00854-8 CCC: $14.00

```
Ac-N-Aib-A-D-Nle-E-A-A-I-K-H-L-A-E-H-Nle-Aib-A-H-
   1                                              19
                                          G-P-V-D
                                         20    23
H2N-G-Aib-R-A-F-A-E-F-H-K-A-L-H-E-A-Nle-H-A-Aib
   42                                             24
```

Figure 1. The amino acid sequence of KO-42 in the one-letter code where A is alanine, D is aspartic acid, E is glutamic acid, F is phenylalanine, G is glycine, H is histidine, I is isoleucine, K is lysine, L is leucine, N is asparagine, P is proline, Q is glutamine, R is arginine, and V is valine. Aib is α-aminoisobutyric acid and Nle is norleucine. The C-terminal is amidated and the N-terminal is acetylated. The sequence is presented to illustrate the solution structure of the hairpin motif.

polypeptides developed from SA-42 were determined by the same techniques, and they, too, folded into helix−loop−helix motifs. Flanking arginine, lysine, and ornithine residues were found to enhance the reactivity of histidine side chains by factors of 5−35, depending on the nature of the flanking side chain and the solvent.[17] Although the rate enhancements were modest, the concept was successful, and we have now explored the use of flanking protonated histidine side chains. In this Article we wish to report that reactive sites with unprotonated histidine side chains flanked by protonated histidine side chains are capable of catalyzing acyl-transfer reactions of reactive esters with second-order rate constants that are more than three orders of magnitude larger than those of 4-methylimidazole. These rate enhancements are the largest so far reported for rationally designed four-helix bundles and pave the way for further development of reactive sites in designed polypeptides capable of substrate recognition and chiral discrimination.

Results

The Design of KO-42. The design of KO-42 was based on the design and solution structure of the template polypeptide SA-42 which folds into a hairpin helix−loop−helix motif that dimerizes in an antiparallel mode to form a four-helix bundle.[4,16] The design of SA-42 has been described in detail, previously.[4] The amino acid sequence of KO-42 (Figure 1) is identical to that of SA-42 except for five residues, His-11, His-19, His-26, His-30, and His-34. The amino acid sequence of KO-42 is varied extensively to allow the assignment of the ^{1}H NMR spectrum, and two phenylalanine residues were incorporated at the lower end of helix II to act as NOE reporter groups and to generate increased shift dispersion in the folded peptide. The choice of amino acids was governed to some extent by the propensity for secondary structure formation,[18] and some artificial amino acids were used.

In the modeled polypeptide the folded states of the amphiphilic helical sequences were stabilized by capping residues, salt bridges, and helix dipole stabilizing residues in agreement with the generally accepted strategy that was recently reviewed by Bryson et al.[1] The C- and N-terminal charges were neutralized by amidation and acylation, respectively. Leucine, isoleucine, norleucine, and phenylalanine residues were incorporated to form shape complementary interfaces between the helices.

On the surface of the folded polypeptide a reactive site was engineered that was designed to catalyze acyl-transfer reactions of esters using the catalytic efficiency of imidazole residues. The designed reactive site contained unprotonated His residues designed to function as nucleophilic catalysts flanked by protonated histidine residues capable of binding one or both of the ester oxygens in the transition state (Figure 2). Positively charged hydrogen bond donors such as Arg, Lys, and Orn have previously been found to provide only modest rate enhancements.[9,14] The ratio of the second-order rate constants, k_2(polypeptide)/k_2(4-MeIm), for the reaction with mono-*p*-nitrophenyl fumarate was typically less than 10 in aqueous solution. In KO-42 flanking histidines were used instead.

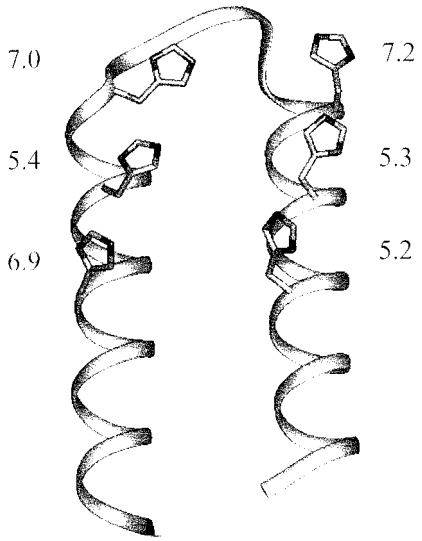

Figure 2. Modeled structure of the hairpin helix−loop−helix motif of KO-42 showing only the side chains of the histidine residues in the reactive site. The measured pK_a values are given next to the residues to which they have been assigned. KO-42 is a symmetric dimer, but only the monomer is shown for reasons of clarity of presentation.

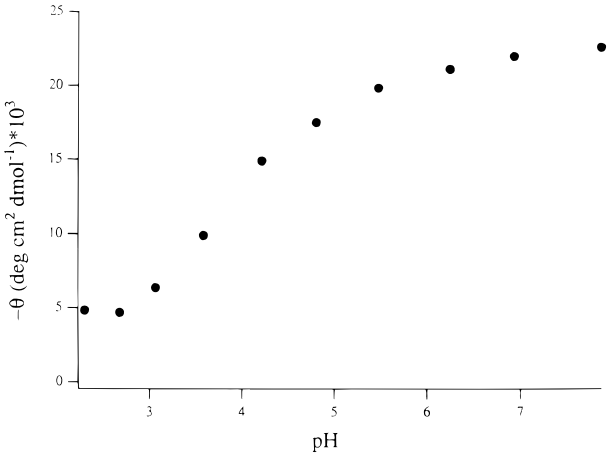

Figure 3. The absolute value of the mean residue ellipticity of KO-42 at 222 nm as a function of pH at ambient temperature. The concentration of peptide was 0.22 mM.

The Solution Structure of KO-42. The CD spectrum of KO-42 is typical of helical proteins[19] with minima at 208 and 222 nm. The mean residue ellipticity at 222 nm was −24 000 ± 1000 deg cm^2 dmol^{-1} in aqueous solution at pH 6.15 and 293 K. The measured ellipticity compares well with that of other reported four-helix bundles and may be used to estimate a helical content of more than 65%.[20,21] The CD spectrum is strongly dependent on pH (Figure 3), and at pH 2.5 the mean residue ellipticity is only −5000 deg cm^2 dmol^{-1}. The effect of temperature on the CD spectrum is weak, the mean residue

(17) Lundh, A.-C.; Broo, K.; Baltzer, L. *J. Chem. Soc., Perkin Trans. 2* **1997**, 209.

(18) Richardson, J. S; Richardson, D. C. *Prediction of Protein Structure and the Principles of Protein Conformation*; Fasman, G. D., Ed.; Plenum Press: New York, 1989; pp 1−88.

(19) Johnson, W. C., Jr. *Proteins* **1990**, *7*, 205.

(20) Chen, Y.-H.; Yang, J. T.; Chau, K. H. *Biochemistry* **1974**, *13*, 3350.

(21) Engel, M.; Williams, R. W.; Erickson, B. W. *Biochemistry* **1991**, *30*, 3161.

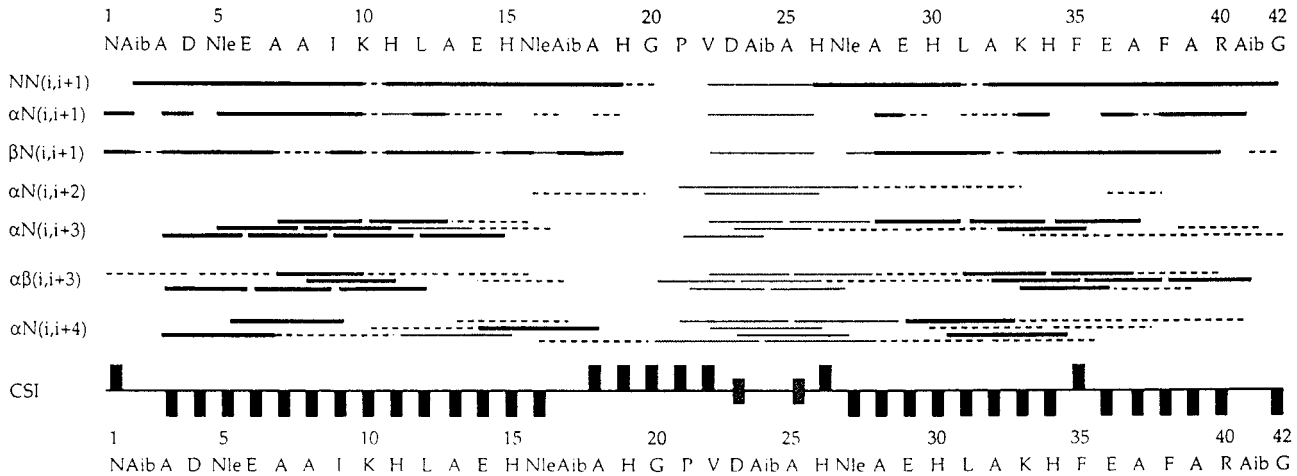

Figure 4. Summary of α proton chemical shifts and interresidue sequential and medium-range NOEs observed in the ^{1}H NMR spectrum of KO-42 in 6 vol % TFE at pH 6.1 and 323 K. "Downward" bars indicate negative deviations of α proton chemical shifts relative to those of random coils which is typical of residues in helical conformations. No bar is given for Aib residues since they have no α protons, and bars for Asp-23 and Ala-25 indicate that they have not been assigned. Solid lines indicate observed NOE contacts between residues, dashed line indicate possible NOE contacts that are unobservable due to overlap, and solid thin lines are drawn for all possible contacts involving residues that have not been assigned. Nomenclature is according to Wutrich.[32]

ellipticity at 323 K is only 15% less than that at 293 K and KO-42 does not have a well-defined melting point. Trifluoroethanol (TFE) increases the absolute value of the mean residue ellipticity in aqueous solution at pH 5.0, and most of the increase takes place in the interval from 0 to 16 vol %. The increase is small, less than 10%, which shows that the secondary structure is well developed already in aqueous solution.

The ^{1}H NMR spectrum of KO-42 has been assigned from the 500 MHz ^{1}H NMR TOCSY and NOESY spectra in 2, 4, and 6 vol % of trifluoroethanol in 90% H_2O 10% D_2O at pH 5.8 and 323 K according to the strategy developed for the structural characterization of SA-42.[4,16] Small amounts of TFE sharpen NMR resonances and simplify assignments but do not induce tertiary structure.[16] The chemical shifts of the α protons in 6 vol % (1.5 mol %) TFE in the sequences 3−16 and 27−42 show negative deviations relative to those of random coils, which is indicative of helical structure[22] (Figure 4). The helical regions correspond closely to those determined for the template polypeptide SA-42, and the fold of the template polypeptide is preserved in spite of the replacement of five residues in the sequence. A number of medium range NOEs typical of helical conformations were observed in the segments 3 −18 and 28 −41. The extent of helix formation is in agreement with the magnitude of the mean residue ellipticity.[20,21] The short segment between residues 18 and 26 is characterized by positive deviations of the chemical shifts in comparison with those of random coils which is typical of β structures, turns, and loops. Because the lack of medium range NOEs suggests a floppy structure these two observations indicate that this segment forms a loop.

Long-range NOE contacts between the aromatic protons of Phe35 and of Phe38 and the methyl groups of Nle-5 as well as those of Ile-9 or Leu-12, or both, were identified (Figure 5) and show the formation of the hairpin conformation as described for SA-42.[4] Close proximity between the upper end of helix I and the lower end of helix II is only compatible with the formation of a hairpin motif. It was established by equilibrium sedimentation ultracentrifugation that KO-42 is a dimer at pH 6 and 293 K with evidence for some higher order aggregates. The experimentally determined molecular weight of KO-42 was

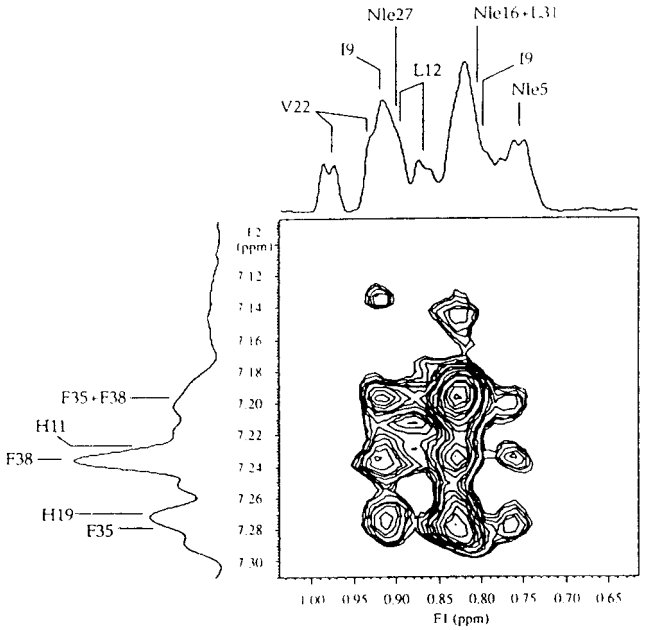

Figure 5. Part of the NOESY spectrum of KO-42 in aqueous solution at pH 5.8 and 323 K showing NOE contacts between Phe aromatic protons and Ile, Leu, and Nle methyl protons. Connectivities between Phe-35 and Phe-38 aromatic protons and the methyl group of Nle-5 demonstrate unequivocally the formation of the hairpin motif. The chemical shifts deviate slightly from those in Table 1 since the solvent is different.

11 000 D which is approximately 20% higher than the calculated molecular weight of the dimer, 8980 D. The ultracentrifugation experiment was also carried out at 303 K, but the difference between the results at the two temperatures was small, less than 5%. The combined results from NMR and CD spectroscopy and ultracentrifugation therefore show that KO-42 folds into a hairpin helix−loop−helix motif that dimerizes to form a four-helix bundle. The interface between the two monomers within the dimer contains mainly alanine residues which makes it hard to identify intermolecular NOEs since alanine methyl groups are not well dispersed and cross peaks appear close to the diagonal in the NOESY spectrum. In the case of SA-42, intermolecular NOEs were unequivocally assigned that showed connectivity between Phe aromatic protons and methyl groups

(22) Wishart, D. S.; Sykes, B. D.; Richards, F. M. *J. Mol. Biol.* **1991**, *222*, 311.

Table 1. Rate Constants for Acyl-Transfer Reactions of *p*-Nitrophenyl Esters at 290 K

	k_2(KO-42) (M^{-1} s^{-1})	k_2(4-MeIm) (M^{-1} s^{-1})	k(uncat)	$\frac{k_2(\text{KO-42})}{k_2(\text{4-MeIm})}$	$\frac{k_2(\text{KO-42})}{k(\text{uncat})}$
		Mono-*p*-nitrophenyl Fumarate			
aq buf pH 4.1	0.10	$8.8 * 10^{-5}$		1140	
10% TFE, pH 4.1	0.052	$8.4 * 10^{-5}$	$1.2 * 10^{-6}$ M^{-1} s^{-1}	620	43000
aq buf, pH 5.1	0.31	$7.4 * 10^{-4}$		420	
aq buf, pH 5.85	0.65	$1.0 * 10^{-2}$		65	
30% TFE, pH 5.85	0.064	$1.2 * 10^{-3}$	$3.7 * 10^{-6}$ M^{-1} s^{-1}	54	
D_2O buf, pH* 6.1	0.68				
D_2O buf, pH* 4.7	0.10				
		p-Nitrophenyl Acetate			
aq buf, pH 5.1	0.29	$7.2 * 10^{-4}$		402	
		D- and L-Tryptophane *p*-Nitrophenyl Ester			
aq buf, pH 5.1	3.7	$5.5 * 10^{-3}$		670	
		Cyclopentane-*trans*-1,2-dicarboxylic Acid Mono-*p*-Nitrophenyl Ester			
aq buf, pH 5.1	0.86	$1.5 * 10^{-3}$		590	

Chart 1

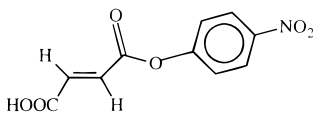

I

in the hydrophobic core and demonstrated antiparallel dimerization. Since the sequence of KO-42 is the same as that of SA-42 except for the replacement of 5 amino acid residues we assume that the mode of dimerization is the same.

The Reactions Catalyzed by KO-42. KO-42 catalyzes acyl-transfer reactions of *p*-nitrophenyl esters (Table 1) and the products of the KO-42 catalyzed reactions of mono-*p*-nitrophenyl fumarate (I) were identified from the ^{1}H NMR spectrum recorded under reaction conditions. In aqueous solution the fumaryl anions were identified as reaction products from the single resonance in the ^{1}H NMR spectrum, and the assignment was verified by the addition of a few crystals of fumaric acid to the NMR tube. At pH 5.5 the resonance was severely broadened suggesting that the fumaryl dianion binds to the polypeptide. Minor amounts, less than 5%, of Bis-Tris ester were detected in 10 vol % TFE when Bis-Tris buffer was used, but in acetate buffer the fumaryl anions were the only observable products.

Under reaction conditions in 10 vol % TFE the spin system of the substrate, the fumaryl monoester (two doublets, $J = 16$ Hz), was replaced by that of the reaction product, a second fumaryl spin system, which was found to be the corresponding trifluoroethyl mono ester. KO-42 therefore catalyzes hydrolysis reactions in aqueous solution and transesterification reactions to form the trifluoroethyl ester in 10 vol % trifluoroethanol (TFE).

ES-MS was used to measure the molecular weight of the peptide after reaction with a 10-fold excess of I at pH 6.1. About 20% of the peptide had become acylated by the fumaryl residue probably through a direct reaction between the reactive ester and a lysine side chain, and the same reaction is also likely to occur with other *p*-nitrophenyl esters. The reactivity of KO-42 was, however, not affected, and acylation does not perturb the function of KO-42. CD spectroscopy was also used to monitor the reaction under conditions of excess substrate, and the mean residue ellipticity did not change. The reaction products obtained were those expected in imidazole catalyzed reactions where an initially formed acyl intermediate reacts with the most potent nucleophile in the reaction solution to form the reaction product. An acyl transfer to the hydroxide ion results in a hydrolysis reaction, and an acyl-transfer to the trifluoroethoxide ion[23] corresponds to a transesterification. Intramolecular acyl transfer to a primary amine has been described previously.[9]

The reactions were conveniently followed by monitoring the formation of *p*-nitrophenol by UV spectroscopy at 320 nm. They followed excellent pseudo-first-order kinetics for more than five half-lives even under conditions of more than a 10-fold excess of *p*-nitrophenyl acetate, and no saturation kinetics were observed in aqueous solution at pH 6.2. When the substrate was mono-*p*-nitrophenyl fumarate some product inhibition due to the interaction between fumarate mono- and dianions and the partly protonated catalyst was detected in the kinetic measurements. As a control experiment the reaction was run at pH 5.85 with 10 vol % TFE in the presence of a 4-fold excess of fumaric acid, mainly in its dianionic form, and the second-order rate constant for the KO-42 catalyzed reaction was decreased by about 20% in comparison with the rate constant measured without added fumaric acid. A 4-fold excess of the leaving group, *p*-nitrophenol, did not affect the reaction kinetics. The observed rate decrease upon addition of fumaric acid agrees well with the NMR spectroscopic observation that KO-42 binds the fumaryl dianion.

The second-order rate constants for the reactions of mono-*p*-nitrophenyl fumarate and *p*-nitrophenyl acetate were determined in all cases from the slopes of the linear plots of 3−6 pseudo-first-order rate constants versus concentration of catalyst. In the presence of added NaCl or fumaric acid the reactions were run only once, and their pseudo-first-order rate constants were compared to those of the corresponding reactions without added salt or acid. The pseudo-first-order rate constants for the reactions of the tryptophane and cyclopentanedicarboxylic acid esters were measured twice, and the rate constants for the background reactions were substracted. Division of resulting rate constants by the total concentration of catalyst gave the second-order rate constant.

The reaction was first order in catalyst which shows that the dimer is the reactive species.

The second-order rate constants for the KO-42 catalyzed hydrolysis and transesterification reactions of *p*-nitrophenyl esters are presented in Table 1, together with those of the 4-methylimidazole catalyzed reactions. The rate constant ratio, k_2(KO-42)/k_2(4-MeIm), is pH dependent, and its value at pH 4.1 for the reaction with mono-*p*-nitrophenyl fumarate is 1140, and at pH 5.1 it is slightly less than half of that, 420. The difference is close to what is calculated from the Brønsted

(23) Oakenfull, D. G.; Jencks, W. P. *J. Am. Chem. Soc.* **1971**, *93*, 178.

Chart 2

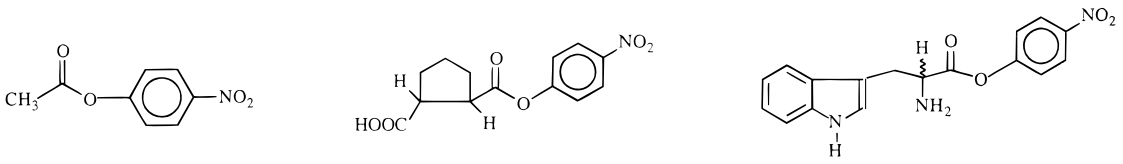

II **III** **IV**

relation and the difference in pK_a values of KO-42 and 4-MeIm using a Brønsted β coefficient of 0.8, as for imidazole catalyzed hydrolysis of *p*-nitrophenyl acetate.[24] The rate enhancement over background in 10 vol % TFE, i.e., over the "uncatalyzed" hydrolysis reaction, is 0.43×10^5, and the rate constant ratio, k_2(KO-42)/k_2(4-MeIm), for the transesterification reaction is 620 in 10 vol % TFE at pH 4.1 and 290 K. These rate enhancements are the largest reported so far for rationally designed four-helix bundle catalysts and are comparable to those observed for typical catalytic antibodies. A number of substrates have been used for acyl-transfer reactions (Table 1), and the similarity in rate enhancements suggests that the recognition of substrates by the catalyst is poor, with regards to positively charged ammonium ions, negatively charged fumaryl residues, and hydrophobic cyclopentyl- and indolyl residues. Alternatively, too many reaction pathways are available in KO-42 catalyzed reactions. The reactivity of KO-42 toward *p*-nitrophenyl acetate can be compared to its reactivity toward I to measure any interaction between reactive site residues of KO-42 and the anionic fumaryl residue of the substrate. The reactivity is very similar for both substrates, and there is therefore little binding of the fumaryl residue by the catalyst.

The pH Dependence of KO-42 Catalyzed Reactions and the Determination of pK_as for the Histidine Side Chains. The dependence on pH of the reactivity of KO-42 was determined, and the observed second-order rate constants showed a strong depencence on pH (Figure 6). A function describing the dissociation of a monoprotonic acid with a pK_a of 5.1 gave the best fit to the experimental results although this is obviously an oversimplification, see Discussion. The side chains of

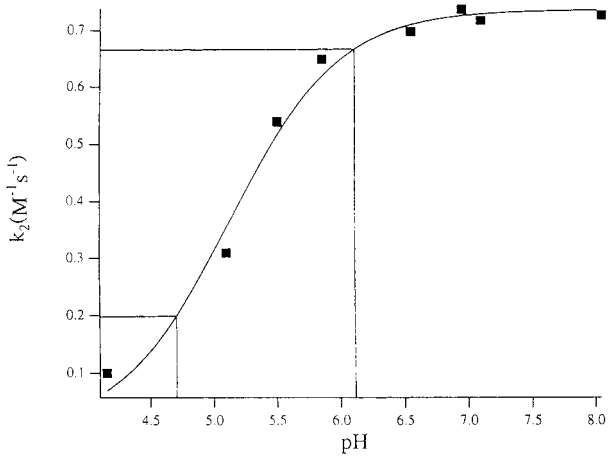

Figure 6. Observed second-order rate constants versus pH for the KO-42 catalyzed reaction of mono-*p*-nitrophenyl fumarate in aqueous solution at 290 K. The solid line describes the dissociation of a monoprotonic acid with a pK_a of 5.1. The function assumes that the catalytic rate of completely protonated KO-42 is 0, but fitting a function where the second-order rate constant is allowed to vary gives a pK_a with a value that differs by only 0.04 pK_a units. The value of the second-order rate constant for the hexaprotonated species obtained under those conditions was 0.02 M^{-1} s^{-1}. The estimate of the second-order rate constants at pH 4.7 and 6.1 for calculation of the kinetic solvent isotope effects are indicated.

noninteracting histidine side chains are expected to have pK_a values of 6.4,[25] and the pH dependence was therefore surprising.

The pK_as of the six histidines of KO-42 were determined from the 1D ^{1}H NMR spectrum at 319 K recorded as a function of pH* in D_2O solution because the resonances were too wide at 290 K to allow the assignment of the ^{1}H NMR spectrum. Imidazole proton chemical shifts of the histidine residues were determined over a range of more than 6 pH units, and at pH 6.1 they were compared to the assignments from the TOCSY and NOESY spectra. A dissociation curve and a pK_a could therefore be assigned to each residue. The effect of temperature on pK_a was estimated to be negligible since the pK_a determination of the 4-methylimidazolium ion at 319 and at 291 K showed a difference that was less than 0.05 pK_a units with the lower pK_a found at the lower temperature. The pK_a values of the histidine residues of KO-42 at 319 K were therefore used in the analysis of the kinetic results at 290 K. The pH titration experiment with KO-42 was also carried out at 291 K in 7 vol % TFE, and the titration curves gave pK_a values that were within 0.1 pK_a units of the ones obtained at 323 K. But the ^{1}H NMR spectrum could not be assigned at 291 K due to line broadening, and the pK_a values could not be unequivocally assigned to individual histidine residues at the lower temperature.

Clear deviations from ideal titration behavior were observed (Figure 7), suggesting strong intramolecular interactions between the histidines, in agreement with the observed pronounced dependence of the mean residue ellipticity on pH. The pK_a values of His-15, His-30, and His-34 determined from the best fits to the experimental results were 5.5, 5.4, and 5.3, respectively, and those of His-11, His-19, and His-26 were 6.5, 6.6, and 7.0 (Figure 7). The best fits of dissociation curves for monobasic acids to the experimental results were obtained for the more acidic histidines, whereas poorer fits were obtained for the more basic histidine residues.

KO-42 can exist in 2^6, or 64, different states of protonation since each one of the six histidine residues can be either protonated or unprotonated. The pH dependence of the CD spectrum shows that different protonation states also have different structures. The observation of nonideally titrating histidines is in fact the observation of the titration of a large number of species with different pK_as. At low pH all histidines are protonated, and as base is added the less basic ones start to titrate, while the more basic ones are still mainly protonated. His-15, His-30, and His-34 titrate, while His-11, His-19, and His-26 are mainly protonated. At a pH where only a small fraction of the more acidic histidines are unprotonated and the other histidines are protonated, they titrate essentially independently of each other. With increasing pH the less acidic ones also titrate to a significant degree, and the latter part of the titration curves of the more acidic ones reflect a composition of a large number of protonation states that are present simultaneously. With the application of a weighting function that emphasizes the early part of the titration curve the obtained pK_a values were 5.4, 5.3, and 5.2 (Figure 8), and these pK_a values were used in the analysis of the pH dependence of the rate constants.

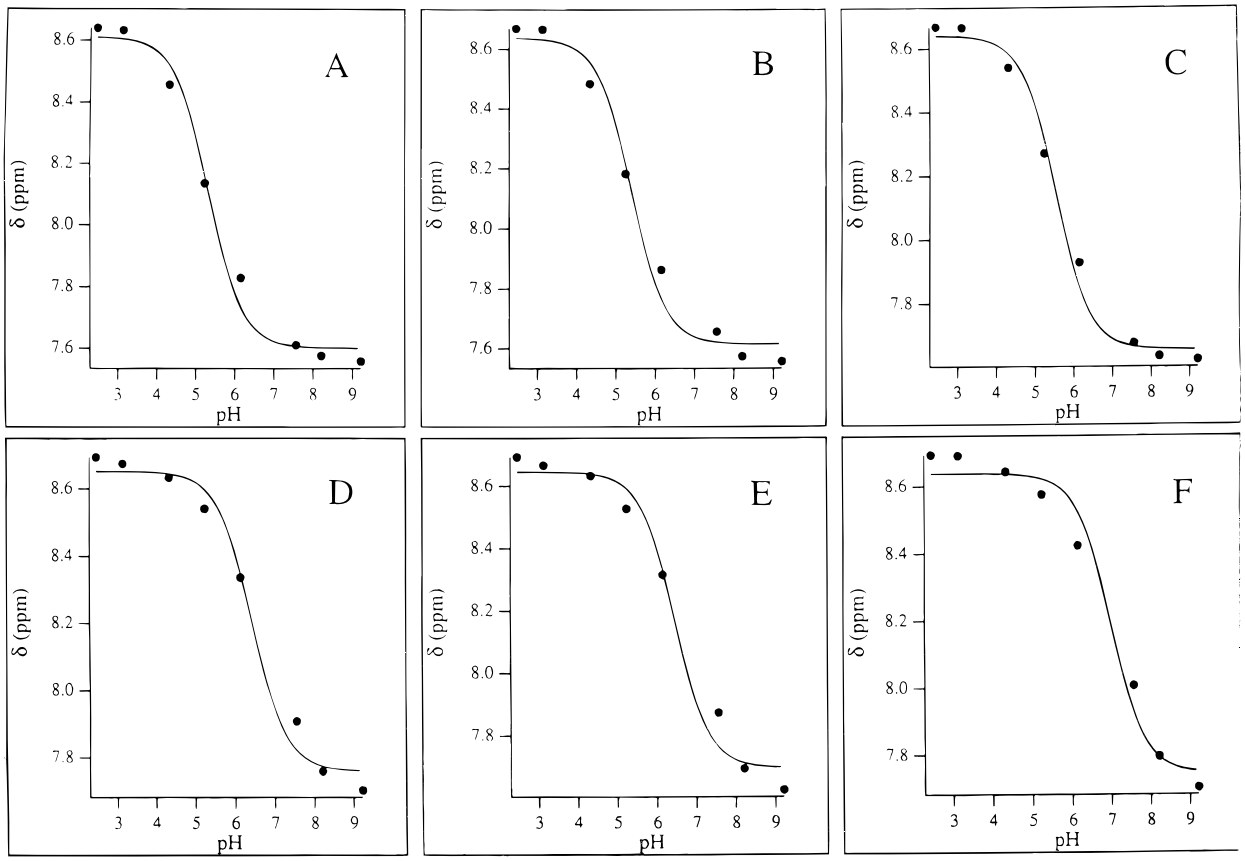

Figure 7. The experimentally determined dissociation curves of the six histidine residue side chains with the best fits to the experimental data of a function describing the dissociation of a monoprotonic acid. Both the chemical shifts of the unprotonated and protonated histidines as well as the dissociation constants were allowed to vary. The pK_a values were 5.3 for His-34 (A), 5.4 for His-30 (B), 5.5 for His-15 (C), 6.5 for His-11 (D), 6.6 for His-19 (E) and 7.0 for His-26 (F).

Strongly nonideal behavior is shown by the more basic histidine residues, but they do not reach their titration midpoints until a pH of almost 7 has been reached. Their pK_as are therefore a pK_a unit or more higher than those of His-15, His-30, and His-34 for all the 64 species in solution. The best fits to the experimental results were obtained for pK_a values of 6.4, 6.5, and 7.0 (Figure 7). Exact pK_a values of His-11, His-19, and His-26 in all the 64 different species are obviously impossible to measure, but the pK_as of the monoprotonated histidine residues in the limiting case when all other histidines are unprotonated are of special interest in the discussion of the nature of the reactive species in the pH independent region. A fit of dissociation curves with weighting functions applied such that the last part is emphasized gives pK_a values of 6.9, 7.0, and 7.2 for the three histidines (Figure 8). These values have been used in the discussion of the identity of the species responsible for the catalysis in the pH independent region.

The Kinetic Solvent Isotope Effect. The pH dependence of the observed second-order rate constant for the KO-42 catalyzed hydrolysis of I showed that the reactive species at low pH had acidic and partly unprotonated histidine residues flanked by more basic and mainly protonated histidines. Further investigations of the role of the flanking residues were therefore carried out by measurements of the kinetic solvent isotope effect for the KO-42 catalyzed hydrolysis of I at pH 4.7 and at pH 6.1 and 290 K. The second-order rate constants in D_2O solution (Table 1) were measured at the reported pH* values, whereas the corresponding second-order rate constants in H_2O solution were estimated as shown in the plot of k_2 versus pH (Figure 6). The pH* in D_2O solution was determined by a glass electrode, and according to the usual convention the pD is obtained by adding 0.4 pH units to the reading on the pH meter, and the D_2O solution is therefore more alkaline than the H_2O solution.

There is, however, also an equilibrium isotope effect on dissociation constants which is mainly due to the fractionation of the lyonium ion, and an acid is therefore less dissociated in D_2O.[26] Since the isotopic fractionation of the imidazolium ion can be neglected,[27] these two effects approximately cancel, and the reaction in H_2O at a given pH can be compared to the reaction in D_2O with the same pH* since the fraction of unprotonated catalyst is the same. The kinetic solvent isotope effect[26] is given by eq 1, where $\prod\phi_R$ is the product of fractionation factors for all exchangeable hydrogens in the

$$k_H/k_D = \prod\phi_R/\prod\phi^\dagger \qquad (1)$$

reactant state and $\prod\phi^\dagger$ is the corresponding product for the transition state. Isotopic fractionation in exchangeable hydrogens arises when the potential well of the hydrogen deviates substantially from that of the solvent, e.g., when it is strongly hydrogen bonded.

The kinetic solvent isotope effect of the KO-42 catalyzed reaction at pH 4.7 is 2.0, and isotopic fractionation must therefore occur in the transition state. Strong hydrogen bonding and/or general acid−general base catalysis is therefore suggested to contribute to the observed rate enhancement. At pH 6.1 the kinetic solvent isotope effect is 1.1 which shows that there is a

(24) Bruice, T. C.; Lapinski, R. *J. Am. Chem. Soc.* **1958**, *80*, 2265.
(25) Tanford, C. *Adv. Protein Chem.* **1962**, *17*, 69.
(26) Laughton, P. M.; Robertson, R. E. *Solute-Solvent Interactions*; Coetzee, J. F., Ritchie, C. D., Eds.; Marcel Dekker: New York, 1969; pp 399−525.
(27) Li, N. C.; Tang, P.; Mathur, R. *J. Phys. Chem.* **1961**, *65*, 1074.

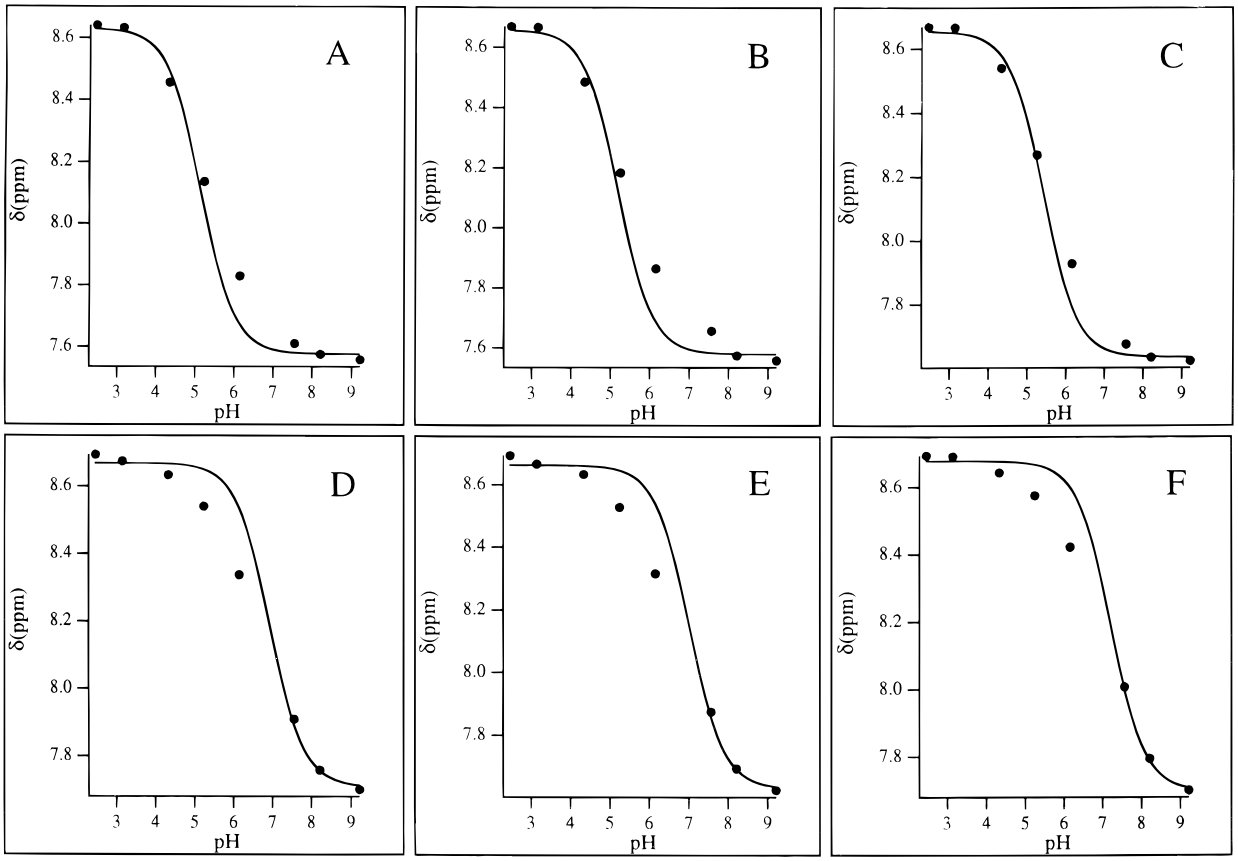

Figure 8. The experimentally determined dissociation curves of the six histidine residue side chains with the best fits to the experimental data of a function describing the dissociation of a monoprotonic acid with weighted points at the early and late stages of dissociation. The pK_a values were 5.2 for His-34 (A), 5.3 for His-30 (B), 5.4 for His-15 (C), 6.9 for His-11 (D), 7.0 for His-19 (E), and.7.2 for His-26 (F).

change of reaction mechanism with pH. No contributions from general base−general acid catalysis or strong hydrogen bonding in the transition state can be observed for the reaction at pH 6.1. The measured kinetic solvent isotope effect at pH 6.1 is the same as that reported for the imidazole catalyzed hydrolysis of *p*-nitrophenyl acetate.[28]

Salt and Solvent Effects on the Reactivity of KO-42. The second-order rate constant determined in 1.0 M NaCl at pH 5.8 was the same, within experimental error, as that determined in aqueous solution without added salt. The second-order rate constants for the KO-42 and 4-MeIm catalyzed reactions were also measured at pH 5.8 in 30 vol % TFE, a less polar solvent than water, and the second-order rate constants were decreased. The ratio of the second-order rate constants, k_2(KO-42)/k_2(4-MeIm), was, however, roughly the same, and charge−charge interactions in the transition state were apparently unimportant or equally important as those in the ground state. In contrast, the relative reactivity of the helix−loop−helix motif RA-42 toward I, k_2(RA-42)/k_2(4-MeIm), was enhanced by almost an order of magnitude in 30 vol % TFE.[17] Flanking histidine residues therefore have a different function at pH 6.1 than flanking Arg, Lys, and Orn.

The effect of the solvent on the structure of SA-42 has been determined previously,[16] and in 30 vol % TFE SA-42 is predominantly a *non*hairpin, helix−loop−helix monomer. Since the magnitude of the rate constant ratio does not decrease more than approximately 20%, one can conclude that the reactive sites are contained within a single helix. It is not yet possible to conclude whether there is one or more reactive sites in KO-42.

(28) Bender, M. L.; Pollock, E. J.; Neveu, M. C. *J. Am. Chem. Soc.* **1962**, *84*, 595.

Discussion

KO-42 catalyzes acyl-transfer reactions of *p*-nitrophenyl esters with second-order rate constants that are more than 10^3 times larger than those of 4-MeIm in aqueous solution. The rate enhancements are comparable to those of typical catalytic antibodies, and the structure and function of the catalyst is therefore of great interest for the further development of *de novo* designed polypeptide catalysts.

The Structure of the Catalyst. KO-42 folds into a hairpin helix−loop−helix dimer as demonstrated by NMR and CD spectroscopy and equilibrium sedimentation ultracentrifugation. Two helical segments and a loop were identified from the α proton chemical shifts and the observed medium-range NOEs (Figure 4), and the magnitude of the mean residue ellipticity at 222 nm was used to calculate a helical content that was compatible with the extension of the helical sequences. Long-range NOEs were used to identify the formation of the hairpin motif (Figure 5), and dimerization was demonstrated by ultracentrifugation. The formation of the hairpin helix−loop−helix motif has been found in all the peptides developed from SA-42 and is not surprising since the residues that form the hydrophobic core of the folded four-helix bundle have been preserved.

The magnitude of the mean residue ellipticity of KO-42 is together with that of SA-42[4] the largest reported so far for a helix−loop−helix motif of this size, and the addition of 16 vol % of the helix inducing solvent TFE does not increase the helical content by more than 10%. The amount of helix formation in KO-42 does not allow for the existence of disordered segments in the two helices so the secondary structures are well defined. The supersecondary structure formation is usually monitored by measuring the concentration dependence of the mean residue

ellipticity, because if the helix−loop−helix dimers dissociate to form monomers its magnitude will decrease. The observation of large negative values for concentrations of KO-42 above 200 μM therefore means that the fraction of monomers is small and that the supersecondary structure of KO-42 is well-defined although the hydrophobic core is not as well packed as that of a native protein. The solution structure of SA-42, the template polypeptide, has been discussed in a similar vein in detail, previously.[4]

At low pH, the helical content of KO-42, unlike that of SA-42, is severely reduced (Figure 3), and the introduced histidine residues, when protonated and positively charged, probably repel each other strongly. The mean residue ellipticity at pH 2.5 is only -5000 deg cm^2 dmol^{-1} which is a value typically found for disordered monomers or random coils with some helix propensity. At high pH when the histidine side chains are largely unprotonated and do not carry any charges, the helical content is high.

The observation of perturbed pK_a values in KO-42 suggests that the histidines interact. When all histidines are unprotonated, the helical content is the highest probably because there is no repulsion due to charge−charge interactions and no intramolecular HisH$^+$-His hydrogen bonding. The secondary structure of KO-42 is the most stabilized when they are all unprotonated. As a result of HisH$^+$−HisH$^+$ interactions the mean residue ellipticity at pH 4.1 is only approximately 65% of that at pH 7. The structure of the reactive species is probably not affected since it contains unprotonated histidines, flanked by protonated histidines, and little repulsion from charge−charge interactions. This is reflected in the magnitude of the second-order rate constant which follows the function describing the dissociation of an acid quite well. It is, however, also possible that it is the neutralizations of the charged aspartates and glutamates that lead to lower helical content.

In the designed motif the histidine residues are located in helical conformations, and each helix contains three residues organized in an almost straight line with a distance between the α carbons of 5.4 Å. It can, however, be seen from the α proton chemical shifts that in the solution structure His-19 is located in the loop region (Figure 4). Its position relative to that of His-15 may therefore not be well defined. His-26 is found in the first turn of helix II, and its orientation relative to His-30 is probably as designed. In helix I a His residue with a depressed pK_a is flanked by two histidines with increased pK_as. In helix II two neighboring residues with depressed pK_a values are flanked on one side by a histidine side chain with an increased pK_a. The organization of unprotonated and protonated His residues as a function of pH is crucial to the reactivity of KO-42.

The Reactivity of KO-42. KO-42 catalyzes acyl-transfer reactions of *p*-nitrophenyl esters in aqueous solution and in mixtures of water and TFE to form the corresponding carboxylic acids and TFE esters. Because the reactive site of KO-42 contains His residues the second-order rate constants of the KO-42 catalyzed reactions have been compared to those of the 4-MeIm catalyzed reactions (Table 1), and in aqueous solution the rate enhancement at pH 4.1 is larger than three orders of magnitude. The second-order rate constants and the second-order rate constant ratio, k_2(KO-42)/k_2(4-MeIm), vary with pH, and in order to assess the efficiency of the catalyst the dependence of rate on pH has been investigated.

The observed second-order rate constant of the KO-42 catalyzed reaction of I increases with pH (Figure 6) and approaches asymptotically a constant value of 0.74 M^{-1} s^{-1}. The second-order rate constant for the 4-MeIm catalyzed reaction approaches a constant value of 1.3 M^{-1} s^{-1}, and the rate constant ratio at high pH is less than 1. The difference in reactivity of the two catalysts is related to the difference in pK_a, as described by the Bronsted relation (eq 2). The pK_a of 4-MeIm is 7.9 and the pK_as of the six histidines of KO-42 in

$$\log k_2 = A + \beta \mathrm{p}K_a \qquad (2)$$

the pH independent region are 5.2, 5.3, 5.4, 6.9, 7.0, and 7.2. The second-order rate constant for a reaction catalyzed by a peptide with six histidine residues may be estimated from the second-order rate constant of 4-MeIm using the pK_a values of 4-MeIm and the six histidines, the Brønsted relation, and a coefficient β of 0.8, which is the value for imidazole-catalyzed *p*-nitrophenyl acetate hydrolysis.[24] Six second-order rate constants were calculated for histidines with the pK_a values of KO-42, and the sum of the rate constants was 0.7 M^{-1} s^{-1} which is very close to the experimentally determined value of 0.74 M^{-1} s^{-1} for the KO-42 catalyzed reaction. In the pH independent region the reactive site of KO-42 therefore functions as six independent histidine residues, and there is no rate acceleration due to cooperative effects between more than one residue.

At pH 4.1 the rate constant ratio in aqueous solution at 290 K is 1140. The magnitude of the observed rate constant ratio is partly due to the difference in pK_a between 4-MeIm (7.9) and the His side chains of KO-42 (5.2 −5.4). The concentration of free base at low pH for 4-MeIm is smaller than for KO-42, but the intrinsic reactivity of 4-MeIm is higher due to its higher pK_a. The net effect at a given pH can be calculated from the Brønsted relation using the coefficient β and the pK_a values of the catalysts. For a β that is less than 1, and a pH that is less than the pK_a values of both catalysts, a weaker base will be a more efficient nucleophile than a stronger base if the total concentrations of catalysts (N + NH$^+$) are the same.[29] From the pK_a values of KO-42 and of 4-MeIm and from the Brønsted relation it can be calculated that for the hydrolysis of *p*-nitrophenyl fumarate at pH 4.1 the KO-42 catalyzed reaction is favored only by a factor of 3.2 over that of 4-MeIm due to the lower degree of protonation. A catalytic factor of 360 is therefore due to transition state binding, assuming that a single dominant catalytic site is active that contains only one of the low-pK_a histidines.

The reactivity of KO-42 toward the *p*-nitrophenyl esters of acetic acid (II), tryptophane (III), and cyclopentane-*trans*-1,2-dicarboxylic acid (IV) was also investigated in aqueous solution at pH 5.1 (Table 1) to explore the possibility of substrate recognition by KO-42. The second-order rate constants vary within a factor of 10, but the rate constant ratio, k_2(KO-42)/k_2(4-MeIm), stays relatively constant in the range from 402 to 670 (Table 1). Binding of the anionic fumaryl residue by the cationic KO-42 would seem likely, but the results do not support such a conclusion as the rate constant ratio is virtually the same for the fumaryl and the acetyl residues. In the tryptophane ester there is a positively charged ammonium group in close proximity to the ester function, but catalysis of the tryptophane ester hydrolysis is not less efficient than that of the fumaryl ester since the rate constant ratio is 670. The catalytic efficiency seems to be rather insensitive to the presence of charged residues in the acetyl residue of the substrate, and it is likely that the charged groups are oriented away from the positively charged flanking residues into the solvent. The reactive site of KO-42 is perhaps instead capable of recognizing hydrophobic groups, since the largest ratios are those of the tryptophane esters and of the cyclopentanedicarboxylic acid monoester. These results

(29) Fersht, A. *Enzyme Structure and Mechanism*; W. H. Freeman and Co.: New York, 1985; pp 47−97.

suggest that catalysts capable of chiral recognition of substrates with hydrophobic groups may be engineered in *de novo* designed proteins.

The pH Dependence of the KO-42 Catalyzed Reaction. There are six histidine residues in KO-42 and therefore 2^6 or 64 different species resulting from all possible combinations of protonated and nonprotonated histidine residues. The plots of chemical shifts of the histidine side chain protons versus pH show that the more acidic ones titrate with pK_a values of 5.5, 5.4, and 5.3 if the best fit of the function describing the dissociation of an acid to the experimental data is used (Figure 7). If weighting functions are applied that emphasize the early parts of the dissociation curve at low pH then these values are decreased by only 0.1 pK_a units and values of 5.4, 5.3, and 5.2 are obtained instead (Figure 8). At pH 4.1 these residues titrate essentially independently of each other since the probability of finding two unprotonated histidine residues in the same polypeptide is less than 10% of the probability of finding a monounprotonated catalyst. The dominant polypeptides at pH 4.1 are therefore, besides the nonreactive hexaprotonated one, three that are pentaprotonated, and they exist in roughly equal amounts due to their similar dissociation constants. The correlation of the reaction rates with the concentration of the pentaprotonated forms of KO-42 show that these are the catalytically active species at low pH. In principle it is possible that all three polypeptides are equally reactive, in which case the reactivity per site is one third of that of KO-42.

Little can be said about the pK_as and reactivities of most of the close to 60 different species that coexist in the pH interval from 5 to 7, except that their combined reactivities appear to add up to a fairly constant value. It is probable that they function through a combination of noncooperative imidazole-like catalysis and cooperative catalysis by flanking protonated and unprotonated histidine residues. The pH dependence for the latter reaction mechanism should give rise to a bell-shaped pH profile because it depends on the coexistence of a nucleophilic histidine in its unprotonated form and a binding histidine in its protonated form. No bell-shaped pH profile was observed, and the explanation is due to the reactivity of the hexaunprotonated form of KO-42.

In the pH independent region in aqueous solution the histidine residues of KO-42 are completely unprotonated, and the pK_a values of the more basic residues were estimated from the latter part of the strongly perturbed dissociation curves through the application of an appropriate weighting function. At high pH the hexaunprotonated species must be the reactive species since it is the only one that is avaliable in significant amounts. Its reactivity can therefore be reliably determined from direct kinetic measurements, and the concentration of that species is readily calculated from the pK_a values of the more basic histidine residues. At a pH above 7.2 it approaches asymptotically the total concentration of peptide, but for pH values below 6.9 it drops off with a rate that approaches the cube of the hydrogen ion concentration. At pH 5.1 the concentration of hexaunprotonated catalyst is in the nM range and catalysis by the hexaunprotonated catalyst is therefore negligible in comparison with that by partially protonated peptides. If the fraction of reaction catalyzed by the hexaunprotonated polypeptide is subtracted from the plot of the second-order rate constant versus pH the resulting pH profile shows a shape that approximates a bell.

The Kinetic Solvent Isotope Effect. The kinetic solvent isotope effect is a measure of whether isotopic fractionation of exchangeable hydrogens occur in the reactant and/or transition states. There is no effect at pH 6.1 in the KO-42 catalyzed reaction of I in aqueous solution, since the rate constant ratio is 1, and general-base catalysis is therefore excluded at that pH, in spite of the fact that there are many unprotonated histidine residues available. The absence of an isotope effect at pH 6.1 shows that there is no fractionation in the transition state and not in the ground state unless they happen to cancel exactly, which excludes the possibility of strong hydrogen bonding between protonated histidine side chains and the developing oxyanion. It shows that at pH 6.1 the dominant reaction mechanism is that of imidazole-like noncooperative catalysis, which is what is found for the hexaunprotonated KO-42.

At pH 4.7 the kinetic solvent isotope effect is 2.0, and there is substantial fractionation in the transition state of the reaction. The observed effect shows that the reaction mechanism is different from that at pH 6.1 and that hydrogens are being transferred or hydrogen bonds are being formed or broken in the transition state since a kinetic solvent isotope effect k_H/k_D that is larger than 1 requires that the fractionation in the transition state is more pronounced than that in the ground state. Fractionation in the transition state is commonly used as evidence for general base catalysis where the water molecule that provides the hydroxide ion is hydrogen bonded to the general base. Since no general base catalysis occurs at pH 6.1, then there is little reason to assume that it does at pH 4.7 where the fraction of unprotonated histidine residues capable of general base catalysis is much smaller. General acid catalysis must however be taken into account as a plausible catalytic mechanism at pH 4.7, perhaps in terms of leaving group protonation. The formation of a strong hydrogen bond to the developing oxyanion is also compatible with the observed isotope effect.

The Function of KO-42. KO-42 catalyzes acyl-transfer reactions of *p*-nitrophenyl esters, and the rate enhancements over the 4-MeIm catalyzed reactions and the reaction mechanism of KO-42 change with pH. At low pH the histidine side chains of KO-42 are protonated to large extents, and the catalytically active species have unprotonated, nucleophilic, histidine side chains flanked by protonated side chains. The pH dependence of the second-order rate constant shows that unprotonated histidines are necessary for the catalytic activity, and the kinetic solvent isotope effect shows that exchangeable hydrogens are strongly hydrogen bonded in the transition state. The initial rate-limiting step of the KO-42 catalyzed reaction at low pH is therefore a nucleophilic attack by a unprotonated His side chain on the carbonyl carbon of the ester to form an acyl intermediate. Transition state binding of one or both of the ester oxygens is provided by a flanking protonated histidine residue. In a second step the acyl intermediate reacts with the most potent nucleophile present to form the reaction product. Under these conditions the rate enhancements are three orders of magnitude over that of the 4-MeIm catalyzed reaction. No acyl intermediate has been detected, in agreement with the fact that spontaneous hydrolysis of acetylimidazole[30] takes place faster than KO-42 catalyzed hydrolysis of I at the concentrations of catalyst used here. Since the first step is rate limiting, the intermediate does not accumulate.

At high pH the reactivity of KO-42 is independent of pH, the second-order rate constant is very close to what is expected from six independent histidine residues and there is no kinetic solvent isotope effect as k_H/k_D is 1 within experimental error. The reaction mechanism is therefore the same as that of imidazole catalysis of ester hydrolysis, and no cooperativity

(30) Oakenfull, D. G.; Salvesen, K.; Jencks, W. P. *J. Am. Chem. Soc.* **1971**, *93*, 188−194.
(31) McMeekin, T. L.; Marshall, K., *Science* **1952**, *116*, 142.
(32) Wutrich, K. *NMR of Proteins and Nucleic Acids*; Wiley: New York, 1985.

between residues is found since there is no rate enhancement over the imidazole catalyzed reaction.

It is not possible to demonstrate whether all three histidine side chains with depressed pK_a values are catalytically active since their pK_a values are very close. If they are all active, the rate enhancement in acyl-transfer reactions due to a nucleophilic His flanked by a $HisH^+$ is a factor of 120 over that of a single His, and a further factor of 3.2 stands to be gained if pK_a values can be designed such that they are depressed as in KO-42. The combination of two histidine residues therefore shows great promise as a concept around which more sophisticated reactive sites can be engineered in the *de novo* design of novel catalysts. Optimism is now called for in the engineering of catalysts capable of substrate recognition, chiral discrimination, and catalysis of reactions for which there are no natural enzymes. The observed rate enhancements are large enough to make screening or selection methods a viable alternative for the further development toward larger rate enhancements and specificity.

Conclusion

We have demonstrated the rational design of a four-helix bundle catalyst capable of catalyzing acyl-transfer reactions of *p*-nitrophenyl esters with rate enhancements that are comparable to those of typical catalytic antibodies. The solution structure has been determined by NMR and CD spectroscopy and ultracentrifugation. The enhanced reactivity is due to cooperativity of unprotonated and protonated histidine residues in a helical segment of the helix−loop−helix dimer. The catalytic efficiency is due to a simple combination of His residues which may prove to be an important concept in the further development of novel catalysts capable of substrate recognition and chiral discrimination.

Experimental Section

The synthesis was first attempted with t-BOC chemistry but with poor results and as a consequence it was instead carried out using FMOC protection groups. The peptide was synthesized on an automated peptide synthesizer from Applied Biosystems using the standard fast FMOC protocol. The amino terminal was capped by acetic anhydride and the carboxy terminal was amidated. The peptide was cleaved from the resin using a mixture of trifluoroacetic acid (4.5 mL), thioanisole (250 μL), ethaneditiol (150 μL), and anisole (100 μL) at room temperature for 2 h. It was precipitated by cold diethyl ether and collected by centrifugation. The peptide was purified by isochratic reversed-phase HPLC on a C-8 semipreparative Kromasil, 7 μ column using 40% isopropyl alcohol and 60% 0.1% TFA, with a flow rate of 5 mL/min. KO-42 eluted as a single peak, and its purity was checked by analytical HPLC on a 5μ Kromasil column under identical conditions except for the flow rate which was 0.5 mL/min. The polypeptide was identified by electrospray MS (calculated 4490, found 4490.6), and the mass spectrum obtained provided a further check on the purity of the peptide since no other peptide peaks were observed.

1D, NOESY, and TOCSY ^{1}H NMR spectra were recorded at 500 MHz using a Varian Unity 500 NMR spectrometer equipped with a matrix shim system MHU 303 from Resonance Research Inc. NOESY and TOCSY spectra were recorded in 90% H_2O/10% D_2O and varying amounts of TFE-d_3 at 323 K with 2 × 256 increments and 16 transients in each increment. The NOESY mixing time was 200 ms, and the TOCSY spin lock was 60 ms. The data were processed using linear prediction and zero filled to 4096 × 2048 data points. The ^{1}H NMR spectrum was assigned in 6 vol % TFE and partially assigned in 2 and 4 vol % TFE to resolve ambiguities.

The apparent molecular weight was determined from the sedimentation equilibrium in a MSE Centriscan analytical ultracentrifuge using a photoelectric scanner at 254 nm. The experimental molecular weight was corrected for calibrated nonlinearity in the detection system and electrostatic repulsion in the salt-free solution. The partial specific volume was calculated from the amino acid composition.[31]

The pK_a values were measured at 319 K (calibrated) by determining the chemical shifts of the H-2 and H-4 protons of the histidine side chains as a function of pH* (uncorr.) in D_2O solution under the usual assumption that the isotope effects cancel out. The experimentally determined dissociation curves formed well resolved plots, and the chemical shifts obtained at pH 6.1 were used to assign the titration curves to individual histidine residues by comparison with the chemical shift assignment at that pH. The ^{1}H NMR spectrum was assigned in 6 vol % TFE and partially in 2 and 4 vol %, and the small observed chemical shift changes upon addition of 2, 4, and 6 vol % (1.8 mol%) demonstrated that the assignment in 6 vol % TFE could be extrapolated to aqueous solution. The temperature dependence of the pK_a of 4-$MeImH^+$ was tested by measuring the dissociation constant at 319 and 291 K, and the obtained values differed by less than 0.05 pK_a units. Samples for NMR spectroscopy were prepared by dissolving lyophilized peptide in the appropriate solvent and adjusting the pH by addition of 0.1 M NaOD or 0.1 M DCl as appropriate. TFE was added by autopipette, and the solution was centrifuged to remove unsoluble impurities. In the TFE titration study the pH was measured in aqueous solution before addition of TFE. The pH is increased by addition of the cosolvent by a few tenths of a pH unit, but the pH was not corrected since the effect of pH on the spectra was negligible.

The pK_a values were determined by fitting an equation describing the dissociation of a monoprotonic acid to the plots of the chemical shifts of the aromatic protons of the His residues versus pH*. The dissociation constant was varied until the best fit to the experimental results was obtained using the Igor Pro software (Wavemetrics Inc.). In order to emphasize the early part of the dissociation curve, the first three and the last two data points were given a weighting coefficient of 3, whereas the other two were not weighted, i.e., a weighting coefficient of 1 was applied. In the fits where the last part of the dissociation curve was emphasized the first two and the last three data points were given the weighting coefficient 3, whereas the other data points were unweighted. The extreme points were used since they provided the chemical shifts of the fully protonated and fully unprotonated species.

CD spectra were recorded on a Jasco-720 spectrometer in the wavelength interval 280 to 200 nm, and the instrument was routinely calibrated with (+)-camphor-10-sulfonic acid.[19] Samples were prepared by diluting aqueous stock solutions by pipetting, and the concentrations of peptide were determined by quantitative amino acid analysis of samples from the stock solutions. The experiments were carried out in 0.1, 0.5, and 1 mm cells, and the temperature dependence of the mean residue ellipticity was measured using a water-jacketed cell together with a circulating HETO constant temperature bath. Sodium acetate buffer was used below pH 5.85, and Bis-Tris buffer was used at pH 5.85 and above, except in the pH titration and temperature experiments where no buffer was used.

Kinetic runs were carried out using Varian Cary 1 and Cary 4 spectrophotometers equipped with Varian temperature controllers by following the absorbance at 320 nm. The kinetic runs with excess substrate were followed at 405 nm due to the strong absorbance at 320 nm. The samples were prepared by dissolving the lyophilized peptide in the reaction solvent, adjusting the pH, and centrifuging the solution prior to transferring it to a 0.1 mm cuvette and typically 300 μL of 0.2−0.4 mM peptide solutions were used.

For kinetic runs with the fumarate and cyclopentanedicarboxylate esters the substrates were weighed and dissolved in the reaction solvent and 20 μL of substrate stock solutions were transferred to the peptide solution. The measurements were started after brief shaking of the cuvette and reintroduction in the thermostatted cell compartment. The *p*-nitrophenyl acetate was poorly soluble in water, and it was therefore dissolved in acetonitrile after which 2 μL of the stock solution was transferred by autopipette to 315 μL of peptide solution. The D- and L-tryptophane esters were dissolved in acetonitrile/buffer 50/50 after which 2 μL was transferred to 315 μL of peptide solution in the cuvette. Substrate concentrations were typically 0.1 mM except under conditions of excess substrate over peptide. The peptide was prepared in a stock solution, and the concentration of that was determined by quantitative amino acid analysis.

The kinetic runs were followed for more than two half-lives and the pseudo-first-order rate constants were determined by fitting a single

exponential function to the experimental data using Igor Pro software. The second-order rate constants for the reactions of mono-*p*-nitrophenyl fumarate and *p*-nitrophenyl acetate were determined by linear regression analysis of the experimentally measured pseudo-first-order rate constants as a function of peptide concentration. The reactions of the tryptophane and cyclopentanedicarboxylate esters were determined by substracting the background reaction from the measured pseudo-first-order rate constant and dividing by the total concentration of peptide ($N + NH^+$). The concentration of peptide was determined by quantitative amino acid analysis. The errors in the rate constants are due to the errors in the regression analysis and the accuracy of the quantitative amino acid analysis, and error limits for individual rate constants are probably $\pm 10\%$.

Acknowledgment. We are indebted to Dr. Christin Choma for the FMOC synthesis of a batch of the peptide and to Dr. Gunnar Johansson for the ultracentrifugation measurements. Financial support from Carl Tryggers Stiftelse and the Swedish Natural Science Research Council is gratefully acknowledged.

JA970854S